



# DEM study of white rice separation in an indented cylinder separator

Xiangyi Meng, Fuguo Jia<sup>\*</sup>, Hualong Qiu, Yanlong Han, Yong Zeng, Yawen Xiao, Peiyu Chen

College of Engineering, Northeast Agricultural University, Harbin, Heilongjiang 150030, China

## ARTICLE INFO

### Article history:

Received 26 September 2018  
Received in revised form 12 February 2019  
Accepted 8 March 2019  
Available online 12 March 2019

### Keywords:

Indented cylinder separator  
Discrete element method  
Escape angle  
Hellinger distance  
Trough position  
Separation efficiency

## ABSTRACT

The precise separation of whole and broken rice is an issue of great significance in rice processing industry. This paper presents a numerical study on the rice separation in an indented cylinder separator based on the discrete element method. The probability density function of escape angle of whole and broken rice was investigated at 10% filling level for various rotational speeds and indent numbers. Hellinger distance, a statistical estimate used to quantify the difference between two probability distributions, was adopted to measure the separation ability. It was found that the Hellinger distance appears to initially increase to a maximum and then decrease with the increase in rotational speed. While the Hellinger distance increases to a maximum value then keeps stable with the increase in indent number. After obtaining the optimal operating condition for the best separation, the position of trough was decided based on the boundary of parabolic trajectories of whole rice after leaving indents. The aim of this work is to determine the best parameters for the indented cylinder separator based on the understanding of separation progress at a particle scale, providing a foundation for the numerical investigation of indented cylinder separator.

© 2019 Elsevier B.V. All rights reserved.

## 1. Introduction

Rice as the staple food is normally consumed in whole milled form [1]. The broken rice is an inevitable problem during the processing. Most consumers prefer whole rice because it has superior nutritional and cooking qualities [2]. Meanwhile, the transaction price of head rice is almost double or triple as compared to that of the broken rice [3]. Therefore, the precise separation is of vital importance for marketing, food quality and food industry requirement. According to the difference in the physical properties of milled rice, such as length, width, shape, density, color *etc.*, mechanical separation and optical sorting are two common separation types. Compared with the high cost and complexity maintenance of optical sorter, the mechanical separation device with simple structure and easy operation is widely used. Whole rice is quite different from broken rice in length compared with width or thickness. Therefore, indented cylinder separator which is the most effective and widely used method compared with screening machine for length separation, has been normally adopted to separate milled rice [4]. The indented cylinder separator is mainly comprised of a cylinder with indents and a trough (Fig. 1). Only the broken rice in the bottom of the rotating cylinder can stay in the indents and be carried up to a certain position, then thrown off and drop into the trough under gravity. While the whole rice which does not fit into the indents cannot be lifted high enough to fall into the trough. They return to the bottom of the cylinder. Thus, the milled rice can be separated into two fractions. The

working principle of the indented cylinder separator is easy to understand. However, previous study showed that the indented cylinder separator needed improvement both in the separation accuracy for whole and broken kernels and in the separation precision for small broken kernels and foreign materials. Therefore, to clarify the effect of engineering and operational factors on the separation ability and appropriately set the processing parameter to achieve an optimal separating efficiency are critically important but very challenging.

A series of studies have been published on finding the optimal operating parameters based on experience, trial and error tests for each machine [5]. Most of the studies were focused on establishing relationships between separation efficiency and operational parameters, including cylinder indent size, revolution speed and trough position [4,6,7]. Concerning the indents shape, Fouad [8] established a new cell configuration through analysis of fall angles of long and short rice. Lee et al. [9] examined the relationship between indents size and the removal rate of broken rice using 41 varieties of milled rice, providing a recommendation for the working diameter. However, these researches are generally difficult to understand the separation process at a particle scale.

A key step in optimizing the separation process is to have an insightful understanding of rice motion. However, to obtain an insight into the rice motion in the cylinder during the separation is difficult using experimental approaches. In order to investigate the particle flow in the cylinder, image analysis has been applied to directly monitor the dynamic motion of particles. Sorica et al. [10] developed a mathematical model of the motion behavior of particles escaping from the indents of the cylinder. Then the kinematic parameters (trajectory, velocity, absolute acceleration) of the working process of the indented cylinder

<sup>\*</sup> Corresponding author.  
E-mail address: [jiafg301@neau.edu.cn](mailto:jiafg301@neau.edu.cn) (F. Jia).

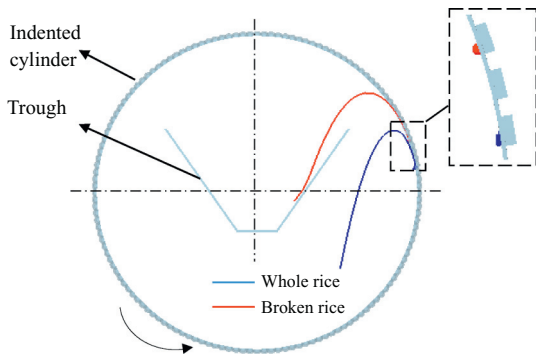


Fig. 1. Cross-section view of an indent cylinder separator.

separator were determined based on the images stored by high speed video camera. The results obtained from experimental research confirm well with the mathematical model. Buus et al. [11] further evaluated the separation efficiency by the statistical method (Hellinger distance) on the basis of Sorica et al. [10]. These two researches provided a novel method for predicting and controlling the separation process, also provided a foundation for this paper. Unfortunately, they were restricted to two dimensions of particle motion. Other experimental methods for the measurement of particle moment, such as positron emission particle tracking (PEPT), and magnetic resonance imaging can only resolve the granular dynamics to a fine scale with relatively poor temporal resolution [12]. Above all, it is expensive, time-consuming and requires a lot of manpower and material resources to conduct experimental studies in the separation process.

Compared with experimental investigations, numerical simulations have proven to be an effective tool for providing new insights regarding the phenomena occurring in food engineering [13–15]. Discrete element method (DEM) proposed by Cundall and Strack [16] have enabled the velocity, stresses and torque to be studied on microscope level and the trajectory of each particle to be visualized on macroscope level [17]. It has been widely used to understand the mechanism of mixing, screening and milling in the simulation of rotating drum or milling device of which the structure is exactly similar to the indented cylinder separator [18–20]. These researches indirectly proved that DEM is an available method. To the best of our knowledge, there is no report available about the application of DEM in the separation process of the indented cylinder separator.

In the current study, the separation process of indented cylinder separator is investigated by the use of DEM. In the first part the numerical and experimental results are compared quantitatively and qualitatively at first. Good agreement is observed in dynamic angle of repose under a range of rotational speeds. The escape angle can be calculated by

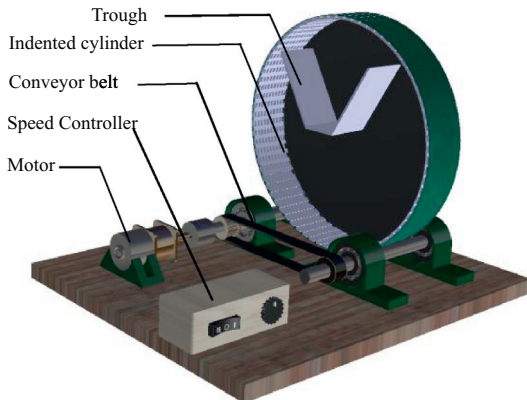


Fig. 2. The CAD model of the indented cylinder separation system.

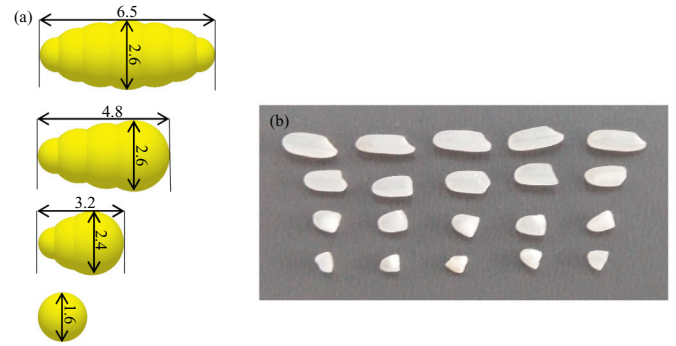


Fig. 3. (a) Multi-sphere model of rice particles used in DEM simulation; (b) Photographs of rice with various length.

obtaining the position of each rice after leaving the indents. Thus, the probability density function of escape angle of whole and broken rice is available. Hellinger distance, a statistical estimate is adopted to quantify the difference between probability distributions of escape angle of whole and broken rice, aiming to evaluate the separation ability. The effect of rotational speed ratio and indent number on the Hellinger distance is investigated. In the second part, the optimal position of trough is decided based on the boundary of whole rice under the optimal condition determined by Hellinger distance. The aim of this work is to determine the best parameters for the indented cylinder separator based on the understanding of separation progress at a particle scale. It not only has the advantage of saving time and material cost but also provides a foundation for the numerical design of indented cylinder separator.

## 2. Simulation method and analysis of separation

### 2.1. DEM model

To simulate the separation of whole and broken rice in an indented cylinder separator, the discrete element method (DEM) has been used. In the present model, the motion of individual particles can be calculated by the Newton's second law of motion, the translational and rotational motions are, respectively, determined by:

$$m_i \frac{d\mathbf{v}_i}{dt} = m_i \mathbf{g} + \sum_{j=1}^{n_i} (\mathbf{F}_{ij}^n + \mathbf{F}_{ij}^t) \quad (1)$$

$$\mathbf{I}_i \frac{d\boldsymbol{\omega}_i}{dt} = \sum_{j=1}^{n_i} (\mathbf{T}_t + \mathbf{T}_r) \quad (2)$$

Table 1

Geometry parameters and physical parameters used in the simulation.

Type	Parameters	Value
Cylinder	Radius × Length (mm)	125 × 50
Indent shape and size	Rectangle Length × Width × Height (mm)	6 × 3 × 3
Rice particle	Density, $\rho_p$ (kg/m <sup>3</sup> )	1550
	Poisson ratio, $\nu_p$	0.25
	Shear modulus, $G_p$ (Pa)	$1 \times 10^6$
	Number of particles	2800 × 4
	Density, $\rho_c$ (kg/m <sup>3</sup> )	7800
Cylinder	Poisson ratio, $\nu_c$	0.3
	Shear modulus, $G_c$ (Pa)	$7 \times 10^8$
	Filling level (%)	10
Particle-particle	Restitution coefficient, $e_{pp}$	0.68
	Coefficient of static friction, $\mu_{spp}$	0.15
	Coefficient of rolling friction, $\mu_{rpp}$	0.01
Particle-cylinder	Restitution coefficient, $e_{pc}$	0.68
	Coefficient of static friction, $\mu_{spc}$	0.1
	Coefficient of rolling friction, $\mu_{rpc}$	0.01
Simulation	Time step, $\Delta t$ (s)	$1.62 \times 10^{-5}$

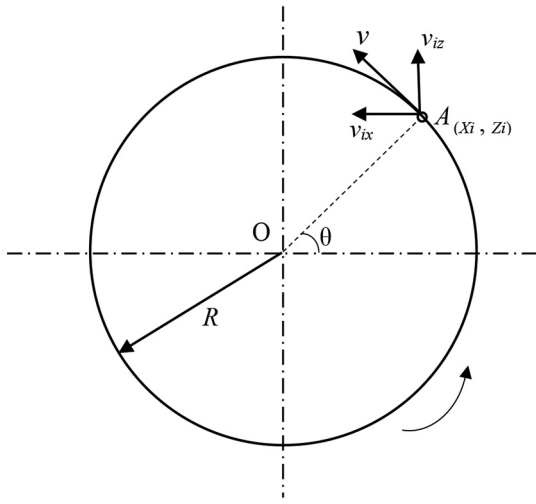


Fig. 4. Dynamic analysis of rice in the cylinder.

where  $\mathbf{V}_i$  and  $\boldsymbol{\omega}_i$  are the translational and angular velocity vector of particle  $i$ , respectively.  $m_i\mathbf{g}$  and  $\mathbf{I}_i$  are the gravity and moment of inertia.  $n_i$  is the number of particle  $j$  in contact with particle  $i$ .  $\mathbf{F}_{ij}^n$  and  $\mathbf{F}_{ij}^t$  are the normal force and the tangential force.  $\mathbf{T}_i$  is the torque caused by the tangential force.  $\mathbf{T}_r$  is the rolling friction torque.

The most popular no-slip Hertz-Mindlin contact model, which combines Hertz's theory in the normal direction and Mindlin's no-slip model in the tangential direction [21], was employed in modeling each contact between particles or particle and geometry. The equations used to calculate the normal total force, the tangential total force, the tangential torque and the rolling friction torque can be found in our previous study [22]. The DEM simulation of rice separation progress in an indented cylinder was performed with a commercial EDEM (DEM Solution Ltd., Edinburgh, UK) software installed on an Intel Core 2 Duo processor with 8 GB RAM and a 64-bit Windows 7 professional operating system. With the current configuration, it takes about 2 CPU hours to simulate 1 s of real time.

## 2.2. Simulation condition

The schematic of the indented cylinder separator system used in the separation is shown in Fig. 2. The system comprises a cylinder with rectangle shape indents and a trough. The axial length of the cylinder is set to 50 mm. Too small of an axial length amplifies wall friction effects. Increasing the thickness, however, brings complications as axial segregation starts playing a role [23]. The cylinder is placed on a pair of rollers which are connected through a timing belt driven by a DC motor. A

PVC belt is used to coat the outside cylinder wall to prevent slippage between the cylinder and the roller. The front faceplate of the rotating cylinder is composed transparent acrylic plate to facilitate visual observations and the other was painted to dark as the background. While in the simulation, in order to simplify the modeling and increase computational efficiency, the drive parts are removed. Note that the coordinate origin is placed in the center of the cylinder front plate.

The multi-sphere model is employed for the representation of rice in different lengths. As can be seen in Fig. 3, rice particles are classified into four groups according to their length. Respectively, whole rice, 3/4 of whole rice, 1/2 of whole rice and 1/4 of whole rice. Head rice is defined as milled kernels that are at least three-quarters of the original kernel length (USDA, 1990) [24]. Therefore, in this study, the first two types of rice are termed as whole rice, and the latter two types of rice are termed as broken rice. The detailed properties of rice particles and geometry are listed in Table 1 based on our previous work [25].

A simulation started with well mixed stable packed bed which the ratio of each particle is equal. Note that the filling level of 10% was investigated, where the filling level is defined as

$$f = \frac{V_{\text{particle}}}{V_{\text{cylinder}}} = \frac{L_{\text{cylinder}} \times A_{\text{particle}}}{L_{\text{cylinder}} \times A_{\text{cylinder}}} \quad (3)$$

with cylinder volume  $V_{\text{cylinder}}$ , volume of the particles  $V_{\text{particle}}$ , depth of drum  $L_{\text{cylinder}}$  and cross-sectional area  $A$ .

The cylinder then rotated at the given condition during the separation process. Unless otherwise specified, all the results were analyzed after 6 s, when the system reached the macroscopically steady state.

## 2.3. Statistical method

### 2.3.1. Escape angle

When the cylinder starts to rotate, rice rises up with the cylinder until it is thrown out, falling along the parabolic trajectory under their own gravity. As seen in Fig. 4, each particle is regarded as a point moving in the cylinder. When the particle reaches escape point, the vertical component of the centrifugal force of the particle is equal to the gravity but in the opposite direction. Assuming the particle is a mass point and ignoring the role of friction, the motion of particle after leaving the indents can be analyzed as follow:

The initial position of particle  $i$  leaving the indent can be described by:

$$X_i = R \cos \theta_i \quad (4)$$

$$Z_i = R \sin \theta_i \quad (5)$$

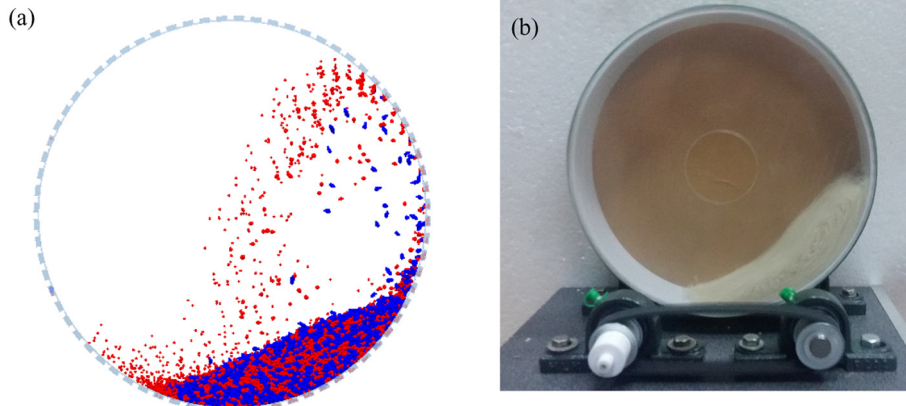


Fig. 5. A snapshot of the simulation and experiment in a steady state.

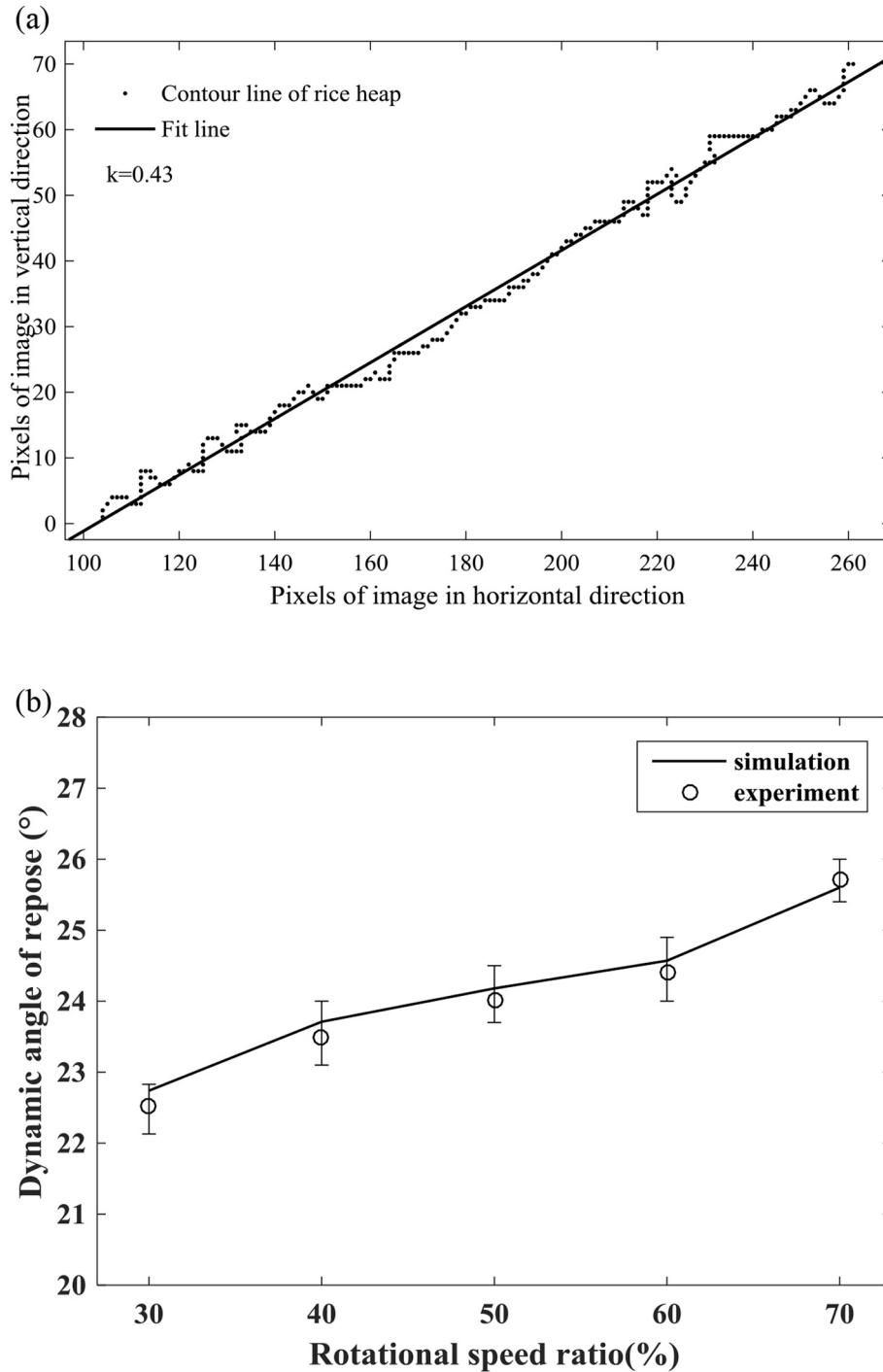


Fig. 6. (a) Numerical measurement of dynamic angle of repose by image processing; (b) Dynamic angle of repose as a function of the rotational speed ratio.

The initial velocity of particle  $i$  is the first derivation of position:

$$v_{ix} = -R\omega \sin\theta_i \quad (6)$$

$$v_{iz} = R\omega \cos\theta_i \quad (7)$$

The ordinate of particle  $i$  at  $ts$  after leaving the cylinder:

$$x_i = X_i + v_{ix}t \quad (8)$$

$$z_i = Z_i + v_{iz}t - \frac{1}{2}gt^2 \quad (9)$$

where  $v_{ix}$  is the initial horizontal velocity of escape point A.  $v_{iz}$  is the initial vertical velocity of escape point A.  $R$  is the radius of cylinder.  $\theta$  is the escape angle.  $X_i$  is the horizontal ordinate of escape point A.  $Z_i$  is the vertical ordinate of escape point A.  $x_i$  is the horizontal ordinate of particle at  $ts$  after leaving the cylinder.  $z_i$  is the horizontal ordinate of particle at  $ts$  after leaving the cylinder.  $g$  is the gravitational acceleration.

Combining Eqs. (4), (5), (6), (7), (8) and (9) gives the following:

$$z_i = R\sin\theta_i + \cot\theta_i(R\cos\theta_i - x_i) - \frac{1}{2}g \frac{(R\cos\theta_i - x_i)^2}{R^2\omega^2 \sin^2\theta_i} \quad (10)$$

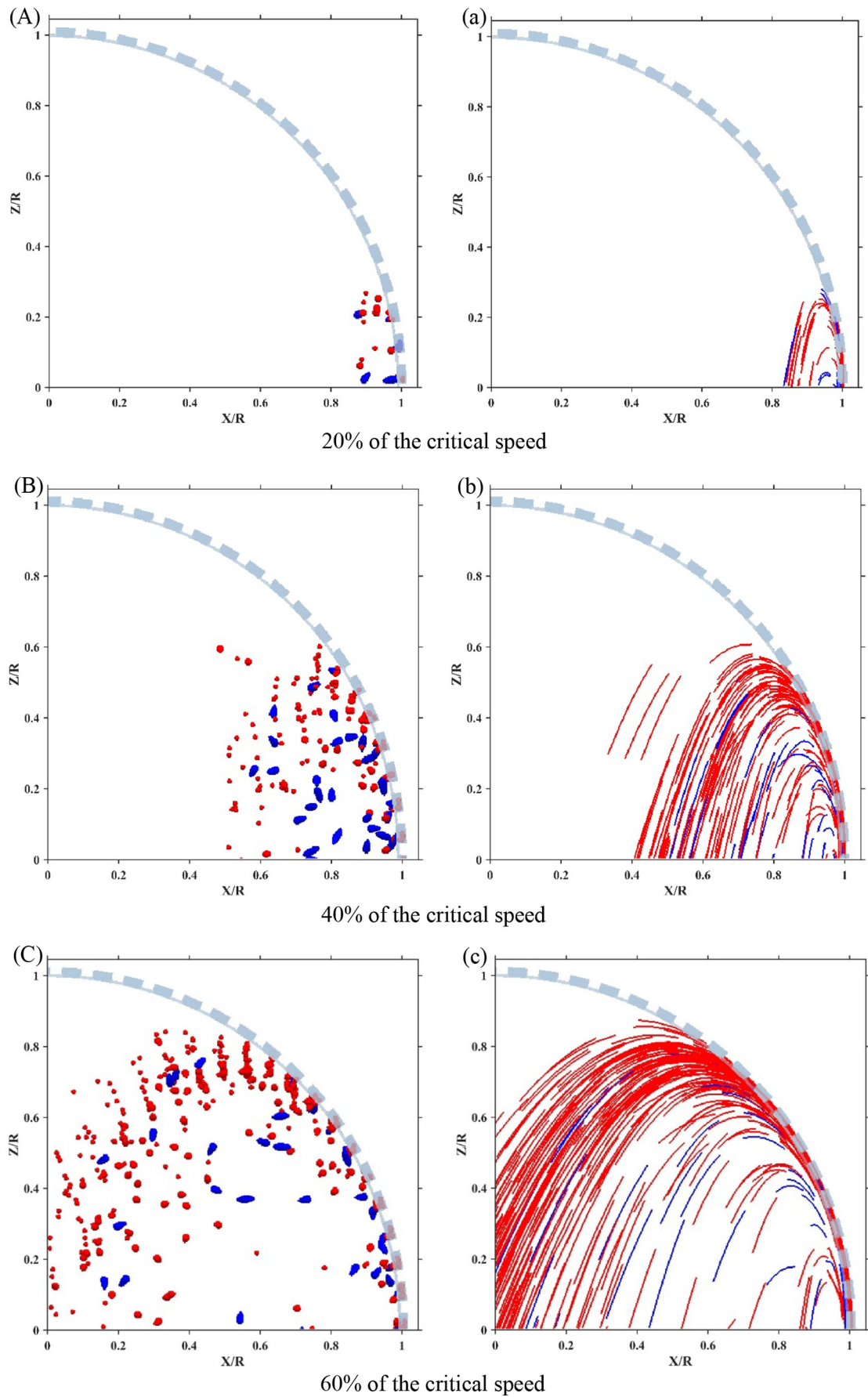


Fig. 7. Snapshots A-E(6 s) and motion trajectory a-e(6–6.05 s) of the whole rice (blue) and broken rice (red) in the cylinder with different rotational speed ratio.

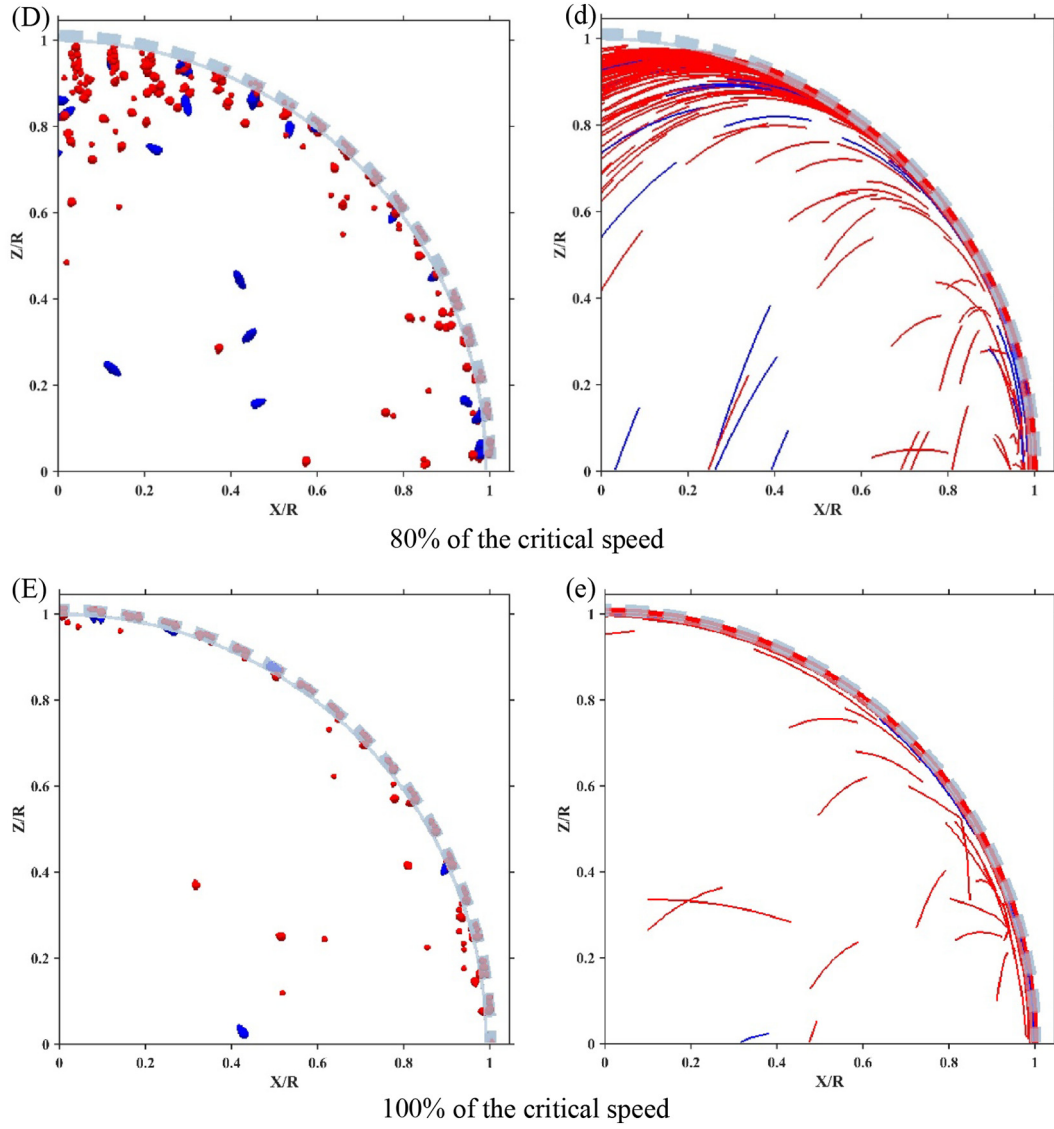


Fig. 7 (continued).

Due to the location of each rice in every timestep can be obtained, the escape angle  $\theta$  can be calculated. First, a function was defined as:

$$f_{\theta} = \left| z_i - R \sin \theta_i - \cot \theta_i (R \cos \theta_i - x_i) + \frac{1}{2} g \frac{(R \cos \theta_i - x_i)^2}{R^2 \omega^2 \sin^2 \theta_i} \right| \quad (11)$$

It becomes a minimization problem:

$$\theta = \operatorname{argmin}(f_{\theta}) \quad (12)$$

Now that the escape angle of each particles is determined, the probability density function of escape angle for two kinds of rice can be calculated.

### 2.3.2. Hellinger distance

The separation ability depends on the difference of escape angle between two kinds of rice. The greater the difference, the smaller the size of overlap between two kinds of rice motion trajectory after leaving the indents, the stronger the separation ability is. In order to evaluate the separation ability, the difference should be quantified. Hellinger distance, a valid statistical estimate which can be used to quantify the

difference between two probability distributions was adopted. The squared Hellinger distance between two probability density function  $p_1(x)$  and  $p_2(x)$  is defined as follows:

$$\operatorname{HD}^2(p_1(x), p_2(x)) = \frac{1}{2} \int (\sqrt{p_1(x)} - \sqrt{p_2(x)})^2 dx \quad (13)$$

The Hellinger distance is a true metric since it is non-negative, symmetric, and satisfies the triangle inequality. It is also bounded between 0 and 1. A distance of 0 corresponds to a complete similarity between two distributions and a distance of 1 to no similarity [26].

The closed form expression of Hellinger distance can easily be computed in the case of normal distributions. For normal distributions,  $p_1(x)$  and  $p_2(x)$  of a random variable  $x$ , where  $p_1 \sim N(\mu_1, \sigma_1^2)$  and  $p_2 \sim N(\mu_2, \sigma_2^2)$ , where  $\mu_1$  and  $\mu_2$  are the means and  $\sigma_1^2, \sigma_2^2$  are the variances for  $p_1$  and  $p_2$ , the Hellinger distance between  $p_1$  and  $p_2$  is given by:

$$H(p_1, p_2) = 4 \left( 1 - \sqrt{\frac{2\sigma_1\sigma_2}{\sigma_1^2 + \sigma_2^2}} e^{-\frac{(\mu_1 - \mu_2)^2}{4(\sigma_1^2 + \sigma_2^2)}} \right) \quad (14)$$

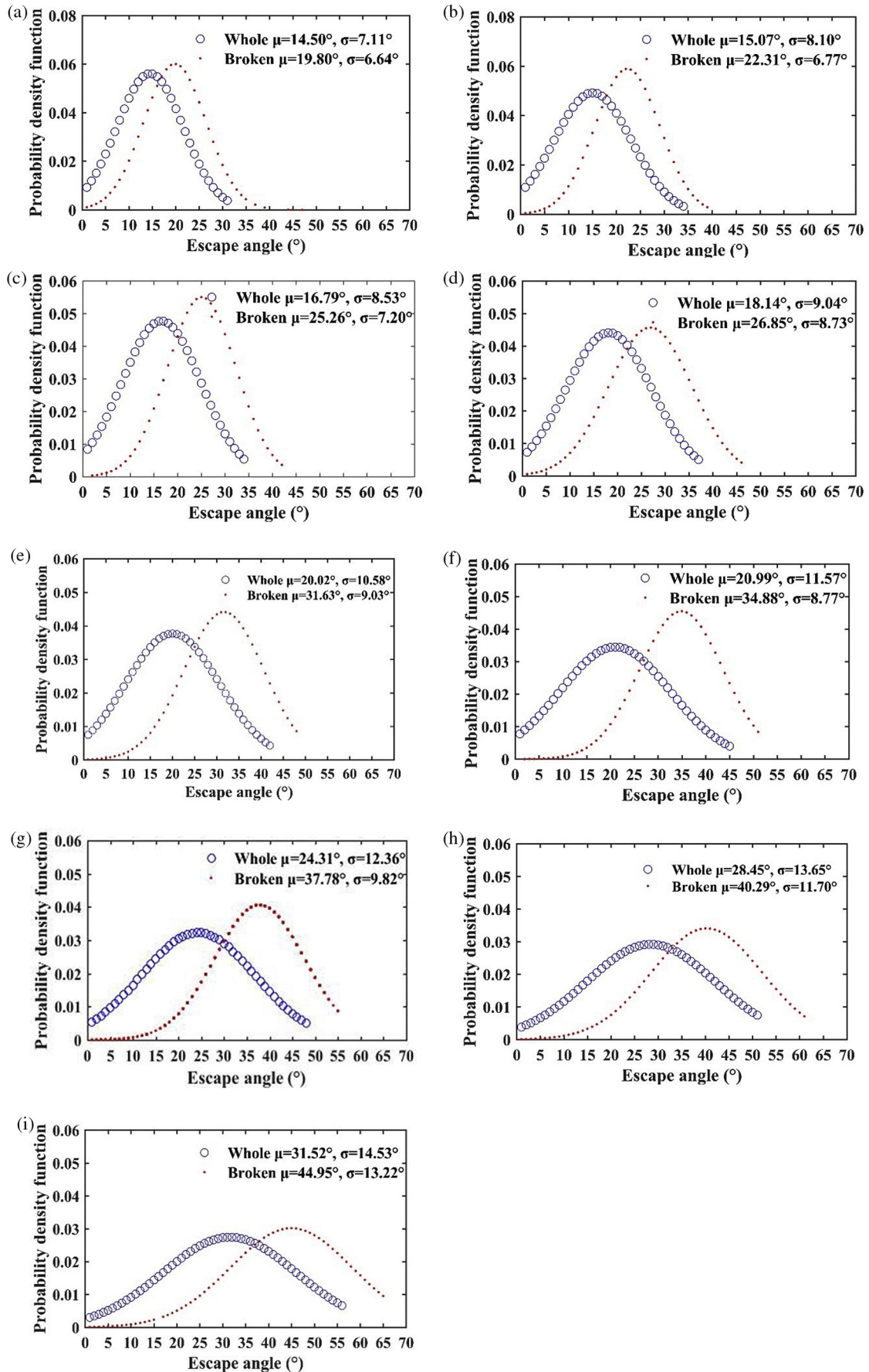


Fig. 8. The probability density function of escape angle under various rotational speed ratio: (a) 30%, (b) 35%, (c) 40%, (d) 45%, (e) 50%, (f) 55%, (g) 60%, (h) 65%, (i) 70% of critical speed when indent number is 72.

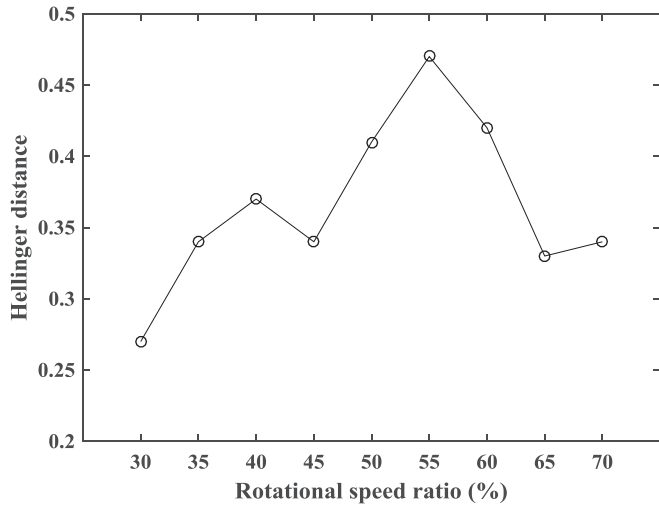


Fig. 9. Variation of the Hellinger distance with rotational speed ratio when indent number is 72.

### 3. Results and discussion

#### 3.1. Model validation

This section investigates the validity of simulation results by comparing the dynamic angle of repose of particle obtained in the DEM simulation with those of a physical experiment. The dynamic angle of repose is defined as the angle between the surface of the bed and a horizontal line. A primary qualitative comparison between experiment and simulation can be obtained from visual inspection. In Fig. 5, the computed dynamic angle of repose is almost identical with the experiment (60% of the critical speed). To give a quantitative comparison, dynamic angle of repose is quantified by image processing technology such as

Fig. 6(a). Details about the image processing method can be found in our previous work [27] and not repeated for brevity. In Fig. 6(b), a quantitative comparison is given by plotting the extracted dynamic angle of repose against the rotational speed ratio. The experiment results are compared to the corresponding simulation results. The bars denote the variation of the measured values under steady-state conditions. It can be seen that the simulation and physical results are quite similar. The trends of the curves are very similar, displaying as the dynamic angle of repose increases linearly with the rotational speed. The result is consistent with those observed by Santos et al. [28]. Thus, one can conclude that the good agreement between the numerical and physical results confirms the validity of the current DEM model.

#### 3.2. Effect of rotational speed on the separation ability

The initial position and motion trajectory of whole and broken rice in the first quadrant under different rotational speeds are shown in Fig. 7, due to the separation mainly occurs here. The snapshots are taken at time 6 s. The blue one represents whole rice and red one is the broken rice. As we can see from Figs. 7(A-E), only few particles can be lifted and they drop off at a low position when the rotational speed is in a lower level, which means a low separation ability. With the increase in the rotational speed, the lifted fraction increases obviously. Compared with whole rice, there are more broken rice lifted. Figs. 7(a-e) shows the motion trajectory of rice from 6 s to 6.05 s which is consistent with the parabolic trajectory. The faster the rotational speed, the larger the escape angle is. The rice is in the centrifugal motion when the rotating speed reaching the critical speed, showing as they stick to the inner surface of the cylinder and remain at relative rest to the cylinder. Separation is therefore no longer possible. From the Fig. 7, it can be concluded that the size of overlap is large between two kinds of rice motion trajectory when the rotational speed is too faster or slower, which means a negative effect on the separation ability.

In order to quantify the variation of escape angle with rotational speed ratio, Fig. 8 shows the normalized probability density

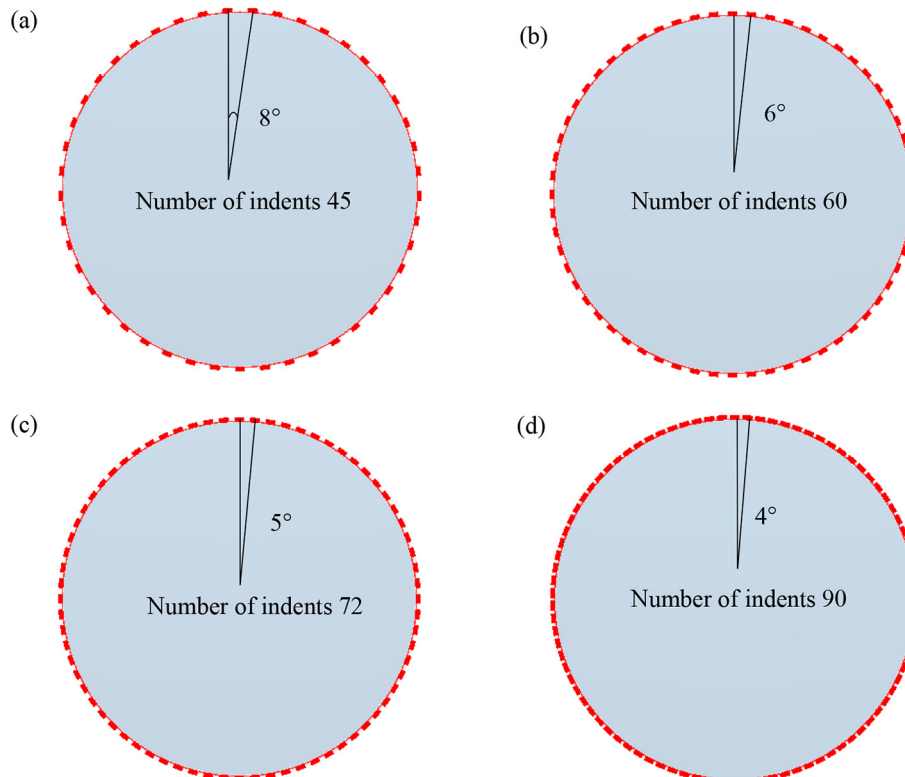


Fig. 10. Cross-section view of an indent cylinder separator with different indent numbers: (a) 45indents; (b) 60indents; (c) 72indents; (d) 90indents.

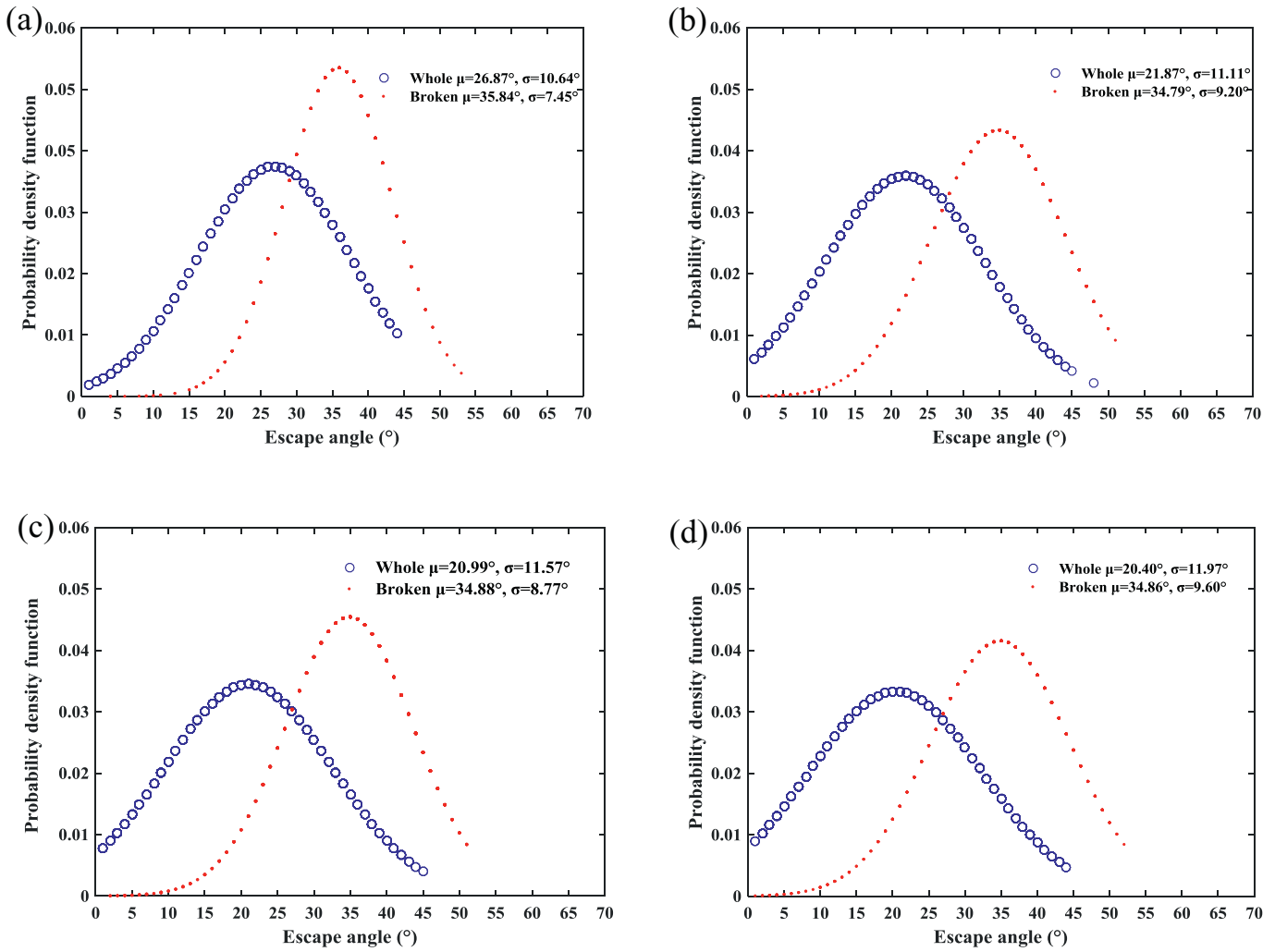


Fig. 11. The probability density function of escape angle under various indent numbers: (a) 45, (b) 60, (c) 72, (d) 90 when rotational speed ratio is 55% of critical speed.

distributions of the escape angle under different rotational speed ratios. It can be seen that with the increase in the rotational speed ratio, no matter whole or broken rice, the peak value moves towards the right, which means the escape angle increases. Meanwhile, the distribution range expands. Due to Hellinger distance can be used to quantify the difference between two probability distribution, Fig. 9 plots the relationship between rotational speed and Hellinger distance. The Hellinger distance appears to initially increase to a maximum and then decreases. The result coincides well with the observation of rice motion trajectory as mentioned above. The maximum value is achieved at rotational speed of 55% of the critical speed which corresponding to the best separation ability.

### 3.3. Effect of indent number on the separation ability

Indent number is an important parameter that needs to be carefully considered in the designing an indented cylinder separator as it will affect particle behavior [29,30]. Therefore, in this section, the effect of the indent number on the separation progress is investigated. The indent number is changing from 45 rows to 90 rows, as shown in Fig. 10.

Fig. 11 shows the normalized probability density distributions of the escape angle under different indent numbers. It can be seen that with the increase in the indent number, no matter whole or broken rice, the peak value moves towards the left, which means the escape angle decreases. Meanwhile, the difference of the peak value increases

between whole and broken rice. This indicates a good separation performance.

The calculated Hellinger distance as a function of the indent number is summarized in Fig. 12. It shows that the Hellinger distance increases

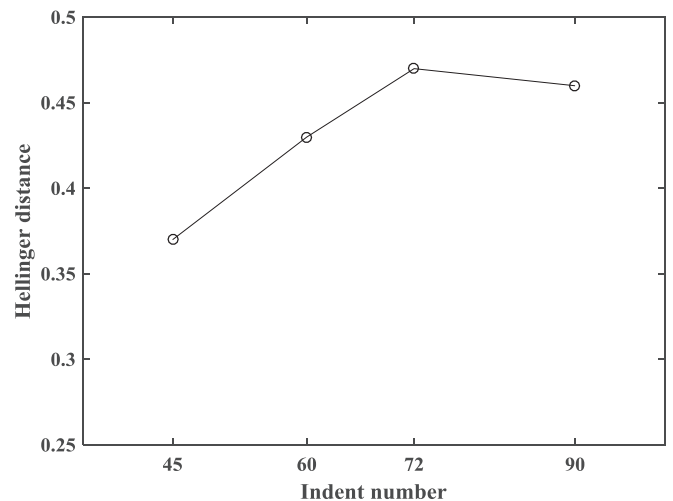


Fig. 12. Variation of the Hellinger distance with indent number when rotational speed ratio is 55% of critical speed.

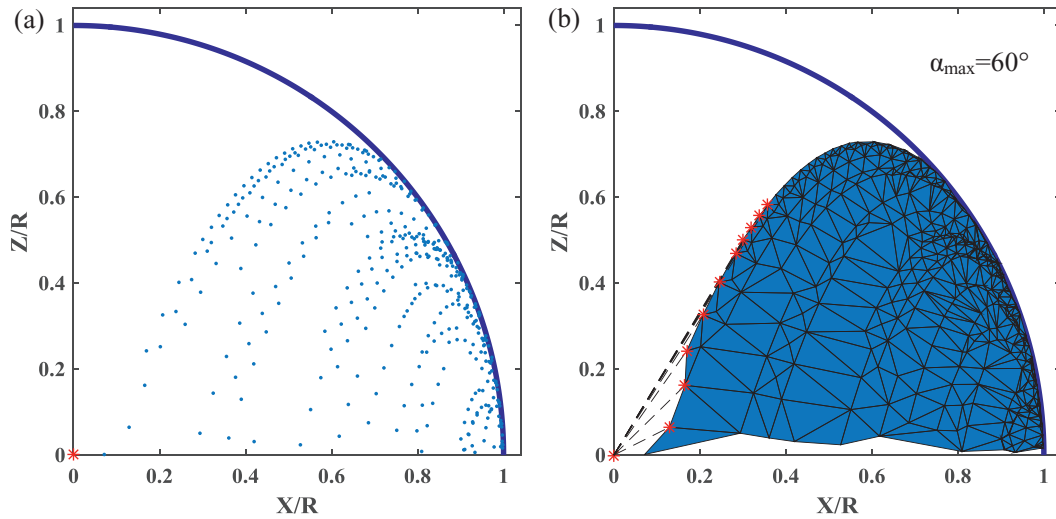


Fig. 13. (a) The position of whole rice under the optimal operating condition from 6 to 6.1 s; (b) The boundary that the whole rice covered from 6 to 6.1 s.

with indent number until a maximum value reached when indent number is 72. With further increase of indent number, the Hellinger distance keeps stable. The lesser indent number means a poor separation ability, while the use of too many indents can not further increase the efficient separation but leads to the higher manufacture cost. Therefore, it is necessary to arrange the number of indents appropriately.

#### 3.4. Determination of the position of trough

Now that the best condition for the separation has been decided based on the above analysis, in order to realize the separation of whole and broken rice, the trough must be placed in an appropriate position. Actually, it is the side of trough which closes to the escape position of rice decided separation ability. It should be placed upper the trajectory of whole rice to prevent the whole rice drop into the trough. Therefore, in this study, the angle of trough was decided based on the trajectory of whole rice under the optimal rotational speed and indent number determined by Hellinger distance.

Fig. 13(a) shows the position of whole rice under the optimal operating condition from 6 to 6.1 s. The boundary was obtained and shown in Fig. 13 (b). Each point on the boundary was connected to the origin of coordinates. The maximum slope of the line between two points corresponding to the optimal angle of trough, which is  $60^\circ$ .

Fig. 14 shows the indented cylinder separator with the trough in optimal angle ( $60^\circ$ ). To quantify the separation ability, the efficiency was calculated as the percentage of separated broken rice in the trough as follows [7]:

$$SE = \frac{N_b T}{N_b S} \quad (15)$$

Meanwhile, the separated whole rice in the trough were calculated as losses as follows:

$$\text{Losses} = \frac{N_w T}{N_w S} \quad (16)$$

where  $SE$  = separation efficiency;  $N_b T$  = number of separated broken rice in trough;  $N_b S$  = number of broken rice in sample;  $N_w T$  = number of separated whole rice in trough;  $N_w S$  = number of whole rice in sample.

It can be seen from Fig. 14 that separation efficiency curve increases rapidly at first but then a light steady increase forms. The maximum value is around 80% which is close to the optimal separation efficiency

with Kim and Park [6] and Lee et al. [9]. Meanwhile, the lifted whole rice can drop into the trough which means the losses is far less than 1%. As we are known, the increase of contact opportunities between broken rice and indents can significantly improve the separation efficiency. At the beginning of the separation, due to the large number of the broken rice, it has more opportunities to get into the indents, showing as the separation efficiency increased sharply. But with further separation, the increasing trend of separation efficiency slows down. One reason is the reduction of the broken rice in the cylinder. And another is due to granular materials that differ in size tend to segregate in the rotary cylinder [31], such as the reverse Brazil nut segregation which may lead to the reduction of the probability of broken rice getting into the indents. Therefore, future work will focus on the effect of the segregation phenomenon of whole and broken rice in the bottom of the cylinder on the separation.

To further verify the optimal trough angle obtained from the simulation. The separation experiments of different trough angles were performed under the optimal rotation speed ratio of 55% of the critical speed. Fig. 15(a) depicts that the separation efficiency with standard deviations at three trough angles of  $55^\circ$ ,  $60^\circ$  and  $65^\circ$ . The obtained results revealed that the separation efficiency decreased by increasing the trough angle. The highest value is almost 0.9 for trough angle of  $55^\circ$ . While Fig. 15(b) indicated that the percentage of lifted separated whole rice. It can be obviously seen that the losses of trough angle of

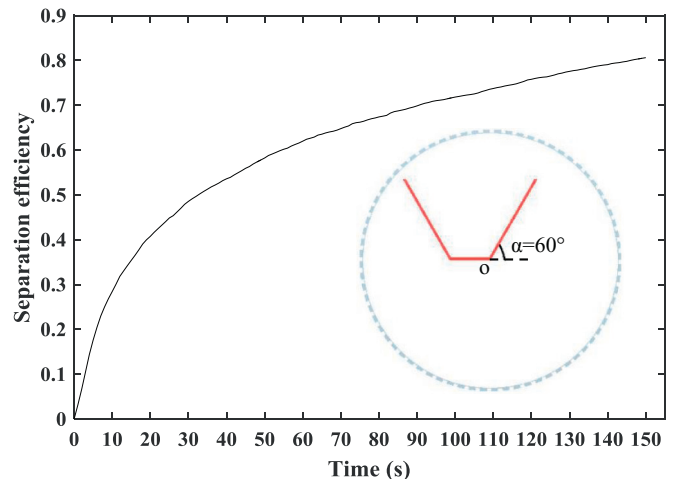


Fig. 14. Separation efficiency as a function of time with optimal position of trough.

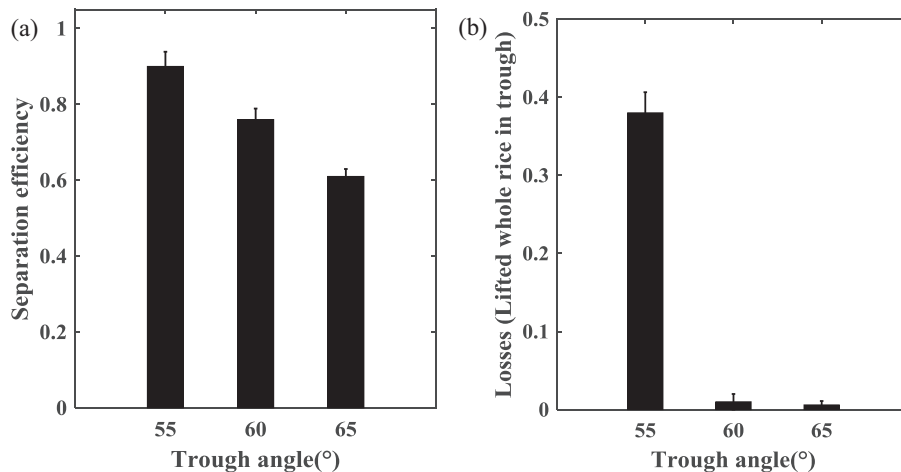


Fig. 15. (a) Separation efficiency at three trough angles; (b) Losses (Lifted whole rice in trough) at three trough angles.

55° is almost reaching 0.4 which is much higher than the trough angle of 60°, showing a terrible separation performance. Hence, the optimum value of trough angle was 60° which gave a value of separation efficiency of 0.78 with a minimum percentage of lifted whole rice in the trough. The optimal trough angle obtained by experiments agreed well with the simulation result, validating the DEM method can be applied to design the indented cylinder separator and achieve optimal performance and better operation parameters.

#### 4. Conclusion

In this study, the separation process of the cylinder separator was very first simulated by the use of DEM. The probability density function of escape angle of whole and broken rice was investigated at 10% filling level for various rotational speeds and indent numbers. Hellinger distance was adopted to evaluate the separation ability. After understanding the effect of rotational speeds and indent number on Hellinger distance, the optimal operating condition for best separation was obtained. Finally, the optimal angle of trough was decided by finding the maximum slope of the line between the connection of whole rice boundary and origin of coordinates. Therefore, a new method to determine the best parameters for the indented cylinder separator by the numerical design was proposed.

The key conclusions are as follows:

- With the increase in the rotational speed, no matter whole or broken rice, the escape angle increases. Meanwhile, the distribution of escape angle became wide. The Hellinger distance appears to initially increase to a maximum and then decrease. The maximum value is achieved at rotational speed of 55% of the critical speed which corresponding to the best separation ability.
- With the increase in the indent number, no matter whole or broken rice, the escape angle decreases. Meanwhile, the difference of distribution of escape angle between whole and broken rice increases. The Hellinger distance increases with indent number until a maximum value then keeps stable.
- The optimal angle of trough can be decided based on the boundary of whole rice. During separation process, the separation efficiency of indented cylinder separator increases sharply at first but then a light steady increase forms. The maximum value is around 80%.

#### Acknowledgements

The authors express their acknowledgment to the Chinese Natural Science Foundation (51575098) for financial support and all of the persons who assisted in this writing.

#### References

- [1] D. Mohapatra, S. Bal, Effect of degree of milling on specific energy consumption, optical measurements and cooking quality of rice, *J. Food Eng.* 80 (2007) 119–125, <https://doi.org/10.1016/j.jfoodeng.2006.04.055>.
- [2] S.A. Mir, S.J.D. Bosco, M.A. Shah, M.M. Mir, S.A. Ganai, Rice: parboiling and milling properties, *Int. J. Food Eng.* 11 (2015) 777–787, <https://doi.org/10.1515/ijfe-2015-0204>.
- [3] B.K. Yadav, V.K. Jindal, Changes in head rice yield and whiteness during milling of rough rice (*oryza sativa*, L.), *J. Food Eng.* 86 (2008) 113–121, <https://doi.org/10.1016/j.jfoodeng.2007.09.025>.
- [4] D.B. Churchill, A.G. Berlage, D.M. Bilsland, Decision-support system development for conditioning seeds with indent cylinder, *Trans. ASAE* 32 (1989) 1395–1398, <https://doi.org/10.13031/2013.31162>.
- [5] C. Sorica, I. Pirna, P. Găgeanu, E. Marin, E. Postelnicu, Indented cylinder separators - quality characteristics expressed as functions of process parameters proceedings of international conference on innovations, recent trends and challenges in mechatronics, *Mechanical Engineering and New High-Tech Products Development - Mecahitech 2011*, p. 11.
- [6] M.H. Kim, S.J. Park, Analysis of broken rice separation efficiency of a laboratory indented cylinder separator, *Korean J. Crop Sci.* 38 (2013) <https://doi.org/10.5307/JBE.2013.38.2.095>.
- [7] M.A. Tawfik, A.M. El Shal, Y.A. El Fawal, Factors affecting the performance of an indented cylinder separator, *Misr J. Agric. Eng.* 28 (2011) 401–415.
- [8] H.A. Fouad, The effect of cell configuration on length grading of beans, *J. Agric. Eng. Res.* 25 (1980) 391–406, [https://doi.org/10.1016/0021-8634\(80\)90080-3](https://doi.org/10.1016/0021-8634(80)90080-3).
- [9] Lee. Choonki, S. Jin, J.T. Yun, S. Jongho, L. Jaeun, K. Jungtae, The optimum operating conditions of indented-cylinder length grader to remove broken rice based on varietal characteristics, *Korean J. Crop Sci.* 54 (2009) 366–374.
- [10] C. Sorica, I. Pirna, C. Bracacescu, E. Marin, E. Postelnicu, Cinematic analysis of particle of impurity in conditioning process of grains into indented cylinder separators, *Engineering for Rural Development - International Scientific Con.* 2012.
- [11] O.T. Buus, J.R. Jørgensen, J.M. Carstensen, Analysis of seed sorting process by estimation of seed motion trajectories, *Image Anal.* (2011) [https://doi.org/10.1007/978-3-642-21227-7\\_26](https://doi.org/10.1007/978-3-642-21227-7_26).
- [12] H. Yang, R. Li, P. Kong, Q.C. Sun, M.J. Biggs, V. Zivkovic, Avalanche dynamics of granular materials under the slumping regime in a rotating drum as revealed by speckle visibility spectroscopy, *Phys. Rev. E Stat. Nonlinear Soft Matter Phys.* 91 (2015), 042206, <https://doi.org/10.1103/PhysRevE.91.042206>.
- [13] C. Gonzálezmontellano, J.M. Fuentes, E. Ayugatéllez, F. Ayuga, Determination of the mechanical properties of maize grains and olives required for use in dem simulations, *J. Food Eng.* 111 (2012) 553–562, <https://doi.org/10.1016/j.jfoodeng.2012.03.017>.
- [14] B.M. Ghodki, T.K. Goswami, Dem simulation of flow of black pepper seeds in cryogenic grinding system, *J. Food Eng.* 196 (2017) 36–51, <https://doi.org/10.1016/j.jfoodeng.2016.09.026>.
- [15] Y. Zeng, F.G. Jia, X.Y. Meng, Y.L. Han, Y.W. Xiao, The effects of friction characteristic of particle on milling process in a horizontal rice mill, *Adv. Powder Technol.* 29 (2018) 1280–1291, <https://doi.org/10.1016/j.apt.2018.02.021>.
- [16] P.A. Cundall, O.D.L. Strack, A discrete numerical model for granular assemblies, *Geotechnique*. 29 (1979) 47–65, <https://doi.org/10.1680/geot.1979.29.1.47>.
- [17] Y.L. Han, F.G. Jia, Y. Zeng, L.W. Jiang, Y.X. Zhang, B. Cao, Effects of rotation speed and outlet opening on particle flow in a vertical rice mill, *Powder Technol.* 297 (2016) 153–164, <https://doi.org/10.1016/j.powtec.2016.04.022>.
- [18] P.Y. Liu, R.Y. Yang, A.B. Yu, Dem study of the transverse mixing of wet particles in rotating drums, *Chem. Eng. Sci.* 86 (2013) 99–107, <https://doi.org/10.1016/j.ces.2012.06.015>.
- [19] H. Komossa, S. Wirtz, V. Scherer, F. Herz, E. Specht, Heat transfer in indirect heated rotary drums filled with monodisperse spheres: comparison of experiments with

- dem simulations, *Powder Technol.* 286 (2015) 722–731, <https://doi.org/10.1016/j.powtec.2015.07.022>.
- [20] B. Cao, F.G. Jia, Y. Zeng, Y.H. Han, X.Y. Meng, Y.W. Xiao, Effects of rotation speed and rice sieve geometry on turbulent motion of particles in a vertical rice mill, *Powder Technol.* (2017) 325, <https://doi.org/10.1016/j.powtec.2017.11.048>.
- [21] A.D. Renzo, F.P.D. Maio, Comparison of contact-force models for the simulation of collisions in dem-based granular flow codes, *Chem. Eng. Sci.* 59 (2004) 525–541, <https://doi.org/10.1016/j.ces.2003.09.037>.
- [22] Y. Zeng, F.G. Jia, Y.X. Zhang, X.Y. Meng, Y.L. Han, H. Wang, Dem study to determine the relationship between particle velocity fluctuations and contact force disappearance, *Powder Technol.* 313 (2017) 112–121, <https://doi.org/10.1016/j.powtec.2017.03.022>.
- [23] N. Jain, J.M. Ottino, R.M. Lueptow, Regimes of segregation and mixing in combined size and density granular systems: an experimental study, *Granul. Matter* 7 (2005) 69–81, <https://doi.org/10.1007/s10035-005-0198-x>.
- [24] USDA, *Inspection Handbook for the Sampling, Inspection, Grading, and Certification of Rice*. HB918–11, Agriculture Marketing Service, 1990 (Washington, DC).
- [25] Y.L. Han, F.G. Jia, Y. Zeng, L.W. Jiang, Y.X. Zhang, B. Cao, Dem study of particle conveying in a feed screw section of vertical rice mill, *Powder Technol.* 311 (2017) 213–225, <https://doi.org/10.1016/j.powtec.2017.01.058>.
- [26] F. Harrou, M. Madakyaru, Y. Sun, Improved nonlinear fault detection strategy based on the hellinger distance metric: plug flow reactor monitoring, *Energy Build.* 143 (2017) 149–161, <https://doi.org/10.1016/j.enbuild.2017.03.033>.
- [27] F.G. Jia, Y.L. Han, Y. Liu, Y.P. Cao, Y.F. Shi, L.N. Yao, Simulation prediction method of repose angle for rice particle materials, *Trans. CSAE* 30 (2014) 254–260 (in Chinese with English abstract).
- [28] D.A. Santos, M.A.S. Barrozo, C.R. Duarte, F. Weigler, J. Mellmann, Investigation of particle dynamics in a rotary drum by means of experiments and numerical simulations using dem, *Adv. Powder Technol.* 27 (2016) 692–703, <https://doi.org/10.1016/j.apt.2016.02.027>.
- [29] A.S.B. Njeng, S. Vitu, M. Clause, J.L. Dirion, M. Debaq, Effect of lifter shape and operating parameters on the flow of materials in a pilot rotary kiln: part iii. up-scaling considerations and segregation analysis, *Powder Technol.* 307 (2016) 415–428, <https://doi.org/10.1016/j.powtec.2016.04.052>.
- [30] X. Bian, G. Wang, H. Wang, S. Wang, W. Lv, Effect of lifters and mill speed on particle behaviour, torque, and power consumption of a tumbling ball mill: experimental study and dem simulation, *Miner. Eng.* 105 (2017) 22–35, <https://doi.org/10.1016/j.mineng.2016.12.014>.
- [31] J.M. Ottino, D.V. Khakhar, Mixing and segregation of granular materials, *Annu. Rev. Fluid Mech.* 32 (2000) 55–91, <https://doi.org/10.1146/annurev.fluid.32.1.55>.